ACS Photonics

Article

pubs.acs.org/journal/apchd5

Electrically-Excited Surface Plasmon Polaritons with Directionality Control

Zhaogang Dong,[†] Hong-Son Chu,[‡] Di Zhu,[†,§] Wei Du,[∥] Yuriy A. Akimov,[‡] Wei Peng Goh,[†] Tao Wang,[∥] Kuan Eng J. Goh,[†] C. Troadec,[†] Christian A. Nijhuis,[∥,⊥] and Joel K. W. Yang*[,†,#]

[†]Institute of Materials Research and Engineering, A*STAR (Agency for Science, Technology and Research), 3 Research Link, 117602, Singapore

[‡]Institute of High Performance Computing, A*STAR (Agency for Science, Technology and Research), 1 Fusionopolis Way, #16-16 Connexis, 138632, Singapore

[∥]Department of Chemistry, National University of Singapore, 3 Science Drive 3, 117543, Singapore

[⊥]Graphene Research Centre, National University of Singapore, 2 Science Drive 3, 117542, Singapore

[#]Singapore University of Technology and Design, 20 Dover Drive, 138682, Singapore

Supporting Information

ABSTRACT: Compact electrical sources of surface plasmon polaritons (SPPs) are promising for integration with high-speed electronics. Being a highly compact source, the point dipole has the ability to directly couple to surface plasmon modes, and be electrically driven through the inelastic tunneling of electrons, for example, at the tip of a scanning tunneling microscope (STM). However, the directional control of electrically excited SPPs from such compact sources has not been demonstrated, despite its importance in controlling the optical energy flow on a chip. In this paper, we present a comprehensive analysis of the directional excitation of SPPs on Au 1D cavity by moving an STM tip relative to the edge of the cavity stripe and analyzing the light collected through an inverted microscope. The directional propagation of the SPP and its far-field emission exhibit a clear cyclic dependence on the relative distance from this edge. These results provide key steps toward realizing compact solid-state devices with the ability to excite and direct the propagation of light.

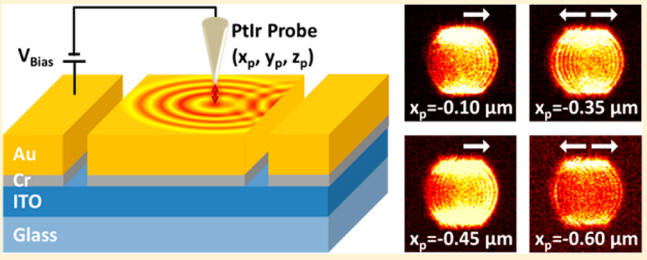

KEYWORDS: *surface plasmon polaritons, directional excitation, electrical excitation, scanning tunneling microscope, dipole source*

The surface plasmon polariton (SPP) is a guided mode of propagating electromagnetic waves at a metal−dielectric interface.[1] SPPs have shown remarkable potential in achieving ultracompact optical waveguiding,[2−4] and nanoscale optical focusing,[5,6] promising for tight integration with CMOS electronics and optical information technology.[7] The directional coupling of free-space optical radiation to SPPs has been thoroughly investigated and demonstrated through a combination of nanostructures and specific illumination strategies.[8−14] Conversely, a separate scheme is needed to achieve directional coupling from electrically driven plasmon sources of which less is known.

Despite being an inefficient process, the inelastic tunneling of low-energy (few eV) electrons accounts for the observation of STM photoemission in early experiments via the excitation of SPPs.[15−17] In contrast to electrical plasmon sources demonstrated with nanomaterials such as silicon nanocrystals,[18] quantum well/nanowire,[4,19−21] organic dyes,[22] or carbon nanotubes,[23] the STM-based excitation does not require quantum emitters, yet enables experiments that probe the position dependence of SPP emission with a highly localized source.[17] It therefore lends itself to convenient modeling as a dipole emitter with a well-defined vertical orientation.[24−26] Recent work has shown the excitation, propagation, scattering, and spatial coherence[27] of SPPs from the tip of an STM on nanostructures,[25,28] and metal surfaces.[27,29] While directional emission in the far field was reported using localized plasmon resonances,[28] the directional coupling to SPPs from an STM tip has yet to be systematically investigated.

In this paper, we theoretically and experimentally investigate the directional excitation of propagating surface plasmons on a periodic 1D cavity by a single dipole source. The directional excitation of SPP was demonstrated numerically using the finite-difference time-domain (FDTD) method, and experimentally with an STM integrated with an inverted optical microscope. The SPP directionality is observed in the Fourier plane (i.e., the back focal plane), where the directional excitation perpendicular to the 1D cavity lines is based on the coherent interference between the STM-excited plasmons and the plasmons reflected off the edges of a single stripe of the 1D cavity. These studies account for the initial steps toward the

Received: November 17, 2014
Published: February 23, 2015

DOI: 10.1021/ph5004303
ACS Photonics 2015, 2, 385−391

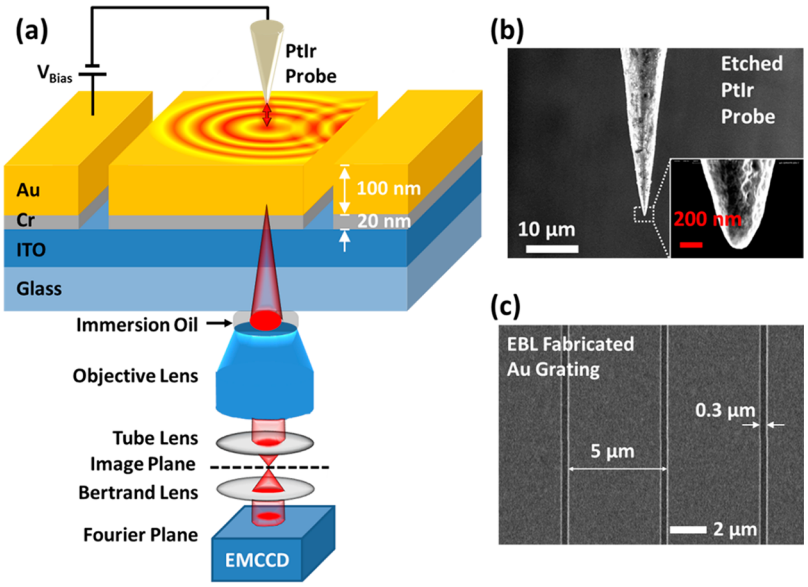

Figure 1. Experimental setup, tip, and sample information. (a) Schematic of the experimental setup for STM-excited plasmons combined with an inverted optical microscope for imaging the SPP directionality in the Fourier plane by a photon-counting electron-multiplying charge coupled device (EMCCD) camera. (b) Scanning-electron micrograph (SEM) images of the electrochemically etched PtIr probe with a ~100 nm radius of curvature. (c) SEM image of the Au 1D cavity patterned by electron-beam lithography (EBL) with a pitch of 5 μm and a gap size of 0.3 μm.

potential implementation of dipole sources of SPPs based on tunnel junctions with controlled directionality, with implications in integrated plasmon sources for optical interconnects.

The experimental setup for SPP excitation by an STM probe is schematically shown in Figure 1a. The STM system is operated under ambient conditions and is integrated with an oil-immersion objective on an inverted optical microscope platform to image the leakage radiation of SPPs.[12,25] Figure 1b shows an SEM image of the STM probe that was fabricated by electrochemical etching of a 0.25 mm diameter PtIr wire (90/10 platinum/iridium) in 33% saturated $CaCl_2$ solution. Figure 1c shows an SEM image of an Au 1D cavity with a pitch of 5 μm and a gap size of 0.3 μm. This 1D cavity sample was fabricated using electron beam lithography (EBL) to reduce line-edge roughness and produce sharp edges. Details of the fabrication process are shown in Figure S1 in the Supporting Information. Unlike previous work where plasmon modes are allowed to propagate on both the top and the bottom surfaces of a thin (35 nm) gold film,[29] here we use optically thick (100 nm) films to limit SPP modes to the top surface. Doing so simplifies the analysis and clearly shows the effects of plasmon reflections from the edges of the film. In addition, we intentionally deposited a 20 nm thick Cr adhesion layer to damp out SPPs on the bottom Au surface. Otherwise, the interference between SPPs on the top and bottom Au surfaces will complicate the interpretation of the optical microscope images.[24,30]

The use of 1D cavity structures enables more light to be collected by the inverted microscope. For comparison, the light collected from a point source of plasmons on a metal film forms a single bright ring when imaged in the Fourier plane.[29] The radius of this bright ring corresponds to the k-vector of the radially propagating SPPs, that is, k_{spp}. On the other hand, due to the periodicity of the 1D cavity, we expect to observe not one but a series of laterally shifted bright ring patterns in k-space instead, as schematically shown in Figure 2b with the zeroth-order plasmon ring indicated. The amount of lateral shift is determined by the pitch Λ of the 1D cavity to be in multiples of $2\pi/\Lambda$. The maximum k-value at the Fourier plane is determined by the numerical aperture (NA) of the objective lens, that is, $|k|_{max} = NA \times k_0 > k_{spp}$, where k_0 is the free-space wavenumber given by $k_0 = 2\pi/\lambda_0$, and λ_0 denotes the free-space wavelength. Another advantage of the 1D cavity is that it acts as a local spectrometer to provide an estimate of the peak wavelength of the emitted light as shown in section 3 of the Supporting Information.

The experimental results in the image and Fourier planes are presented in Figure 2d–f, respectively, where the STM probe was at the center of a single metal stripe as indicated by the red dot in Figure 2d. We used a bias voltage of 2 V, a tunneling current of 50 nA, and an integration time of 300 s for the image plane and 120 s for the Fourier plane. The EMCCD camera was from Princeton Instruments, ProEM$^+$ 512B Excelon 3, set at a multiplication gain of 1000×. Similar to previous reports,[25] the efficiency of electron-photon conversion is estimated to be $\sim 10^{-5}$ based on the image in Figure 2d. The inset shows SPP interference fringes due to the SPPs reflected from 1D cavity edges. These fringes are not to be interpreted as interference patterns of SPPs on the top surface, as that would not be visible to the inverted microscope at the bottom. Instead, it is due to the interference of light scattered through the gaps in the 1D cavity, as detailed in the Supporting Information, Figure S2. These results show that the SPPs maintain coherence as they propagate to the edges of a single 1D cavity stripe and scatter into photons.

The Fourier plane image in Figure 2e shows the expected multiple plasmon rings in k-space that is not to be confused with the real-space interference pattern of Figure 2d. To verify, a smaller 1D cavity pitch will cause these rings to be spaced further apart in k-space (Figure 2f). The main plasmon ring also has a noticeably higher intensity, presumably due to the reduced SPP intensity as it "hops" across the cavity gaps. Upon closer inspection of Figure 2e, we notice that the edges of the rings are brighter on the right half, indicating a preference for right-propagating SPPs. This slight asymmetry is also observed in the image plane in Figure 2d and is likely caused by the

DOI: 10.1021/ph5004303
ACS Photonics 2015, 2, 385–391

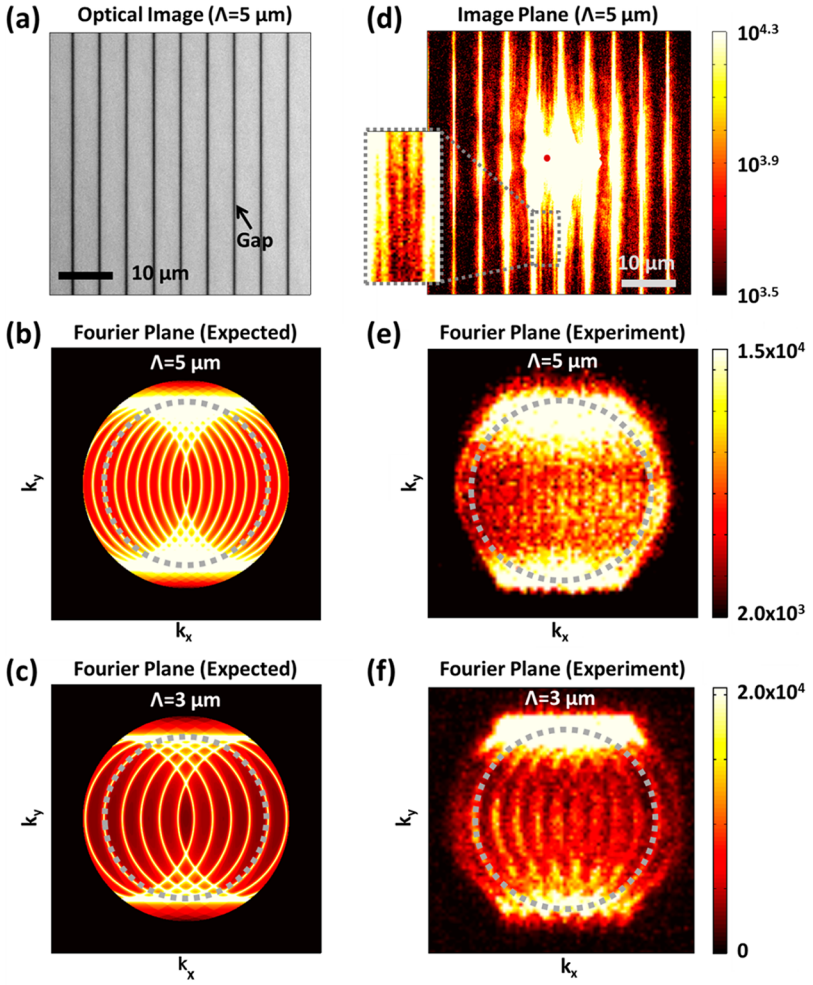

Figure 2. Optical microscope images of the sample and SPP emissions, at both the image and Fourier planes. (a) Optical micrograph of the 1D cavity structure (pitch Λ of 5 μm) with illumination from the bottom. (b, c) Expected Fourier plane image when the STM probe is placed on a 1D cavity structure with a pitch size of 5 and 3 μm, respectively. The 1D cavity causes the central plasmon ring (dashed line) to be repeated along k_x in steps of $2\pi/\Lambda$. The numerical aperture of the oil-immersion lens is 1.30, which allows imaging beyond the central ring. (d–f) Experimentally captured images in the image and Fourier planes due to the scattered light from STM-excited plasmons, imaged in a darkened enclosure. Interference fringes inset demonstrates coherence of plasmon source. The STM probe was placed near the central position of a metal stripe as indicated by the red dot in (d). The unit of intensity is "number of photons".

shape of the probe.[29] The Fourier plane image enables a quantitative measure of the SPP directionality, which will be the focus in the following sections.

To first develop physical intuition, we refer the reader to analysis in the Supporting Information (i.e., Figure S3) for SPP reflections off a single edge of a semi-infinite Au film. As shown in Figure 3, we present numerical simulation results for plasmon propagation from a single dipole source on a 1D cavity structure with a pitch of 5 μm and a gap of 0.3 μm. Two monitors suspended 5 nm above the Au film are introduced to record the intensity of left- and right-propagating SPPs, as indicated in Figure 3a. The directionality factor is defined as the intensity ratio of SPPs arriving at the monitors from the dipole source location after traveling for two 1D cavities. In the analysis, the dipole is positioned closer to the right edge, as shown in Figure 3c–e. As for the case of reflection off a single edge, Figure 3b similarly shows a clear cyclic dependence of the directionality factor when plotted against the dipole's distance from the right edge. In Figure 3c, we observe that a dipole positioned only 100 nm from the right edge will result in SPPs propagating with an almost symmetric profile about the source, that is, with SPPs propagating across two strips (and two gaps) to the right and two strips (only one gap) to the left. Remarkably, shifting the dipole position an extra 150 nm away from the edge causes the plasmons to preferably propagate to the left, crossing three strips and two gaps from the source (Figure 3d). A further shift of 150 nm reverts the directionality to the initial case, as seen in the similarity between Figure 3c and Figure 3e. Therefore, an active control of SPP directionality on Au 1D cavity can be achieved by shifting the dipole-position with respect to the 1D cavity edge to affect the constructive versus destructive interference of SPPs due to reflection from the right edge. Interference due to reflected SPPs from the left edge can be neglected as it propagates over a greater round trip distance > 8.5 μm (e.g., $x_p = -0.4$ μm), compared to the SPP from the right edge. As a result, this SPP component will be too attenuated or incoherent to interfere with the SPP at the dipole position.

Here, we would like to emphasize that it is not surprising that the SPP pattern would be biased toward the right given that the dipole source is located close to the right edge of the stripe. Hence, plasmons propagating to the left edge would have

DOI: 10.1021/ph5004303
ACS Photonics 2015, 2, 385–391

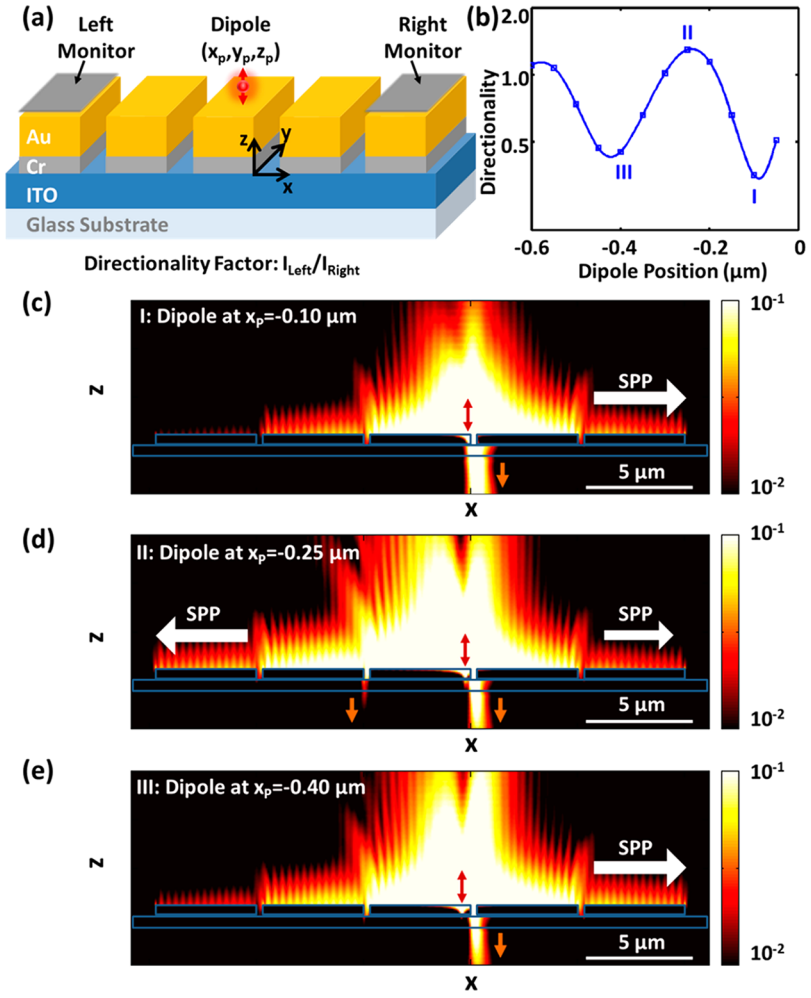

Figure 3. Numerical simulation of plasmons propagating on Au 1D cavity as a function of the dipole-position. (a) Schematic of the FDTD simulations. (b) Dependence of directionality factor on the dipole-position in log scale. (c–e) Electric field intensity $|E|^2$ distribution in the x–z plane when the dipole is at different positions. The red arrow represents the position of the dipole source. Note that by shifting the dipole position by only 150 nm from (c) to (d), we achieve a constructive interference for the left-propagating plasmons resulting in higher intensity of SPPs to the left almost three cavity lines away, and more light scattered through the left gap to the far field as indicated by the orange arrows.

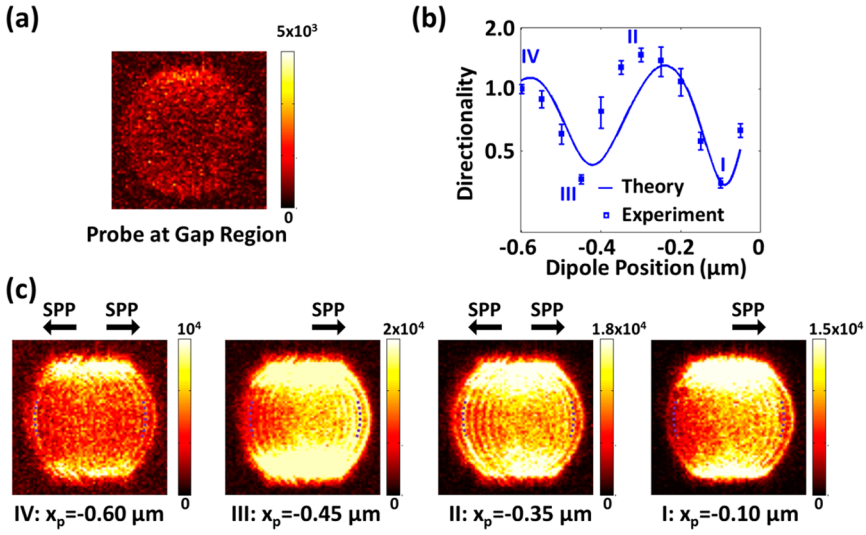

Figure 4. Experimental results demonstrating the directional excitation of SPPs on an Au 1D cavity. (a) Fourier plane image showing isotropic photoemission from ITO when the STM probe was parked in the gap between two cavity lines. (b) Directionality factor as a function of the probe-position for both theory and experiment in log scale. (c) Series of Fourier plane images showing the turning on and off of SPPs propagating to the left at different probe positions.

DOI: 10.1021/ph5004303
ACS Photonics 2015, 2, 385–391

experienced more attenuation than to the right. Furthermore, there is insufficient destructive interference from reflection off the far edge to stop plasmons from propagating to the right. The results therefore show that it is the plasmons propagating to the left that is being modulated by the shift in tip position. Lastly, we would like to mention that there exists a region with high field intensity in the glass substrate as shown in Figure 3c, where such high field intensity was caused by the dipole's localized direct emission penetrating through the air gap.

Here, we present experimental results on the dependence of SPP's directionality on the STM probe-position as predicted above. We first scanned the STM probe to determine the sample topography and the exact location of the 1D-cavity edge, set as "x_p = 0 μm". In order to ensure a sufficient signal level for all Fourier plane images, the tunneling current was set to 50 nA. As a control, the STM probe was first placed into the 0.3 μm wide gap region to probe the weak electroluminescence of ITO and establish the expected isotropic emission. The corresponding Fourier plane image is shown in Figure 4a. No plasmon ring pattern was observed as the ITO−air interface does not support SPPs. A series of Fourier plane images were then captured at 50 nm steps away from the edge, a sampling of which is shown in Figure 4c. These experimentally captured photon mappings are consistent with the simulation results in Figure 3c−e. The directionality factor was determined by taking the intensity ratio between the SPP propagating toward left versus right, obtained from the intensity values in the zeroth-order plasmon ring of the Fourier plane (details in the Methods section). Figure 4b shows a good agreement between the experimental results and the numerical simulations, based on three sets of independent measurements. The cyclic dependence of the SPP's directionality on the probe-position is seen in both experiments and simulations, validating that the SPP directionality could indeed be tuned by varying the position of the probe relative to a 1D cavity edge.

The close correlation between theory and experiment shows that the far-field emissions (measured in experiment) are linked to the near-field SPPs (determined in simulations) on the 1D cavity lines, where the detailed theoretical analysis on this correlation between near-field SPPs and far-field emission is shown by the "near-to-far-field transformation" simulation in the Supporting Information, Figure S6. In addition, there exists a positional shift of maxima II and minima III in Figure 4b, between the numerical simulations and experiments, where the reason for causing such a position shift still remains unknown and the detailed investigations on this position shift might be interesting enough for deserving further studies in the future. Moreover, we show only results at ∼10% of the cavity (i.e., x_p = 0 μm to x_p = −0.6 μm), because the largest directionality control occurs in this region. As we can see from the simulation results in Figure 3, the directionality factor is expected to approach unity when the dipole source is moved away from the edge. Such a reduction in modulation visibility is due to the propagation loss of the reflected SPP from cavity edge. As a result, the reflected SPP will become too weak to interfere with the one at the STM tip position. Partial coherence characteristic of STM-excited plasmon, as explained later, is another parameter to cause the reduced visibility when the STM tip is moved away from the cavity edge. Furthermore, we observed also that the optical intensity of the STM-excited plasmon was not constant when the probe was scanned across different locations of the Au film, due to the dependence on the inelastic-tunneling efficiency to local variations due to surface roughness.[31] However, by extracting the directionality factor we could consistently compare data from different positions on the 1D cavity.

The directionality control was achieved due to the interference of the SPP originating from the STM tip with its reflection predominantly from the right edge (see Figure S3). The demonstrated SPP directionality achieved here has an extinction ratio of ∼2.6:1. Note that, while the directionality achievable by optical excitation is higher,[9,10] this work serves as a demonstration of directional emission of SPPs from electrically-excited dipole sources. The amount of modulation in the directionality factor could be further improved by optimizing the 1D cavity structure, for example, to achieve constructive interference from one edge but destructive interference from the other. For instance, Figure S7 shows simulation results of a 1D cavity with a smaller pitch that exhibits a ∼4.8:1 extinction ratio. Moreover, in the FDTD simulations, the SPP source was modeled as a monochromatic dipole. A more comprehensive analysis can be carried out by considering that the photoemission from the STM tip has a broad spectrum[25,29] with a coherent length of ∼4 μm[27,32] to further improve the correlation between the simulated and measured directionalities. Furthermore, the peak wavelength of the spectrum can be estimated from the Fourier plane image from the 1D cavity structures as explained in Section 3 of the Supporting Information. The peak wavelength could also be tuned by adjusting the bias voltage between tip and sample, Figure S4.[33]

In summary, we investigated the directional coupling of electrically excited plasmons from a position-tunable STM probe on a single stripe of a 1D-cavity structure. Remarkably, as the probe approaches the stripe edge, the SPP propagating away from that edge can be turned "on" or "off" by adjusting the distance of the probe to the edge, achieving constructive or destructive interference with the reflected SPP. While we have focused on Au 1D cavity structures in this work, we expect similar effects to be observed in other materials and geometries such as curved edges and nanostructured arrays for beaming SPPs in various directions.[26] The STM in this study readily provides point sources of SPPs that allows detailed characterization of waveguide designs for optical interconnects aimed at integrated plasmonic circuits.[34] Combined with the local resonances of the metallic nanostructures, and its voltage-controlled spectral response, a wide degree of tunability can be achieved using STM-excited plasmons for advanced characterization of devices.

METHODS

Electron Beam Lithography. The periodic Au 1D cavity sample was fabricated using electron beam lithography (EBL), and the fabrication process is shown in Figure S1a−d in the Supporting Information. Figure S1a presents the sample profile before EBL. A 130 nm thick indium−tin-oxide (ITO) layer was first deposited (ULVAC Solciet evaporation system with a base pressure of 1 × 10^{-5} Pa) onto a glass substrate, where this ITO layer works as a conductive layer for STM. Cr layer with a thickness of 20 nm was then evaporated onto the ITO layer by using electron-beam evaporator (a pressure of 5 × 10^{-5} Pa and a deposition rate of 0.5 Å/s). Next, poly(methyl methacrylate) (PMMA) resist (950k molecular weight, 3.3% wt in anisole) was spin-coated onto glass at a spin speed of 3k revolutions-per-minute (rpm) to give a ∼180 nm thick PMMA layer. The PMMA resist was then baked at 180 °C for 120 s to remove the

DOI: 10.1021/ph5004303
ACS Photonics 2015, 2, 385−391

residue stress and solvent. After that, hydrogen silsesquioxane (HSQ) resist (6% wt in methyl isobutyl ketone) was spin-coated onto the substrate at a speed of 5k rpm to give a ∼80 nm thick HSQ layer. Next, the sample was exposed by EBL (Elionix ELS-7000, electron acceleration voltage of 100 keV, beam current of 150 pA, and dwell time of 1.8 μs). Then, the sample was developed by using NaOH/NaCl salty solution (1% wt/4% wt in deionized water) for 60 s and immersed inside the deionized water for 60 s to stop the development,[35] followed by RIE (reactive-ion-etching) O_2 plasma etching of PMMA (Oxford Instruments Plasmalab 80 Plus, pressure of 62 mTorr, O_2 flow rate of 20 sccm, RF forward power of 100 W, etching time of 60 s),[36] evaporation of 100 nm Au using electron-beam evaporator (pressure of 5×10^{-5} Pa, and an evaporation rate of 0.5 Å/s), lift-off process (*N*-methyl-2-pyrrolidone at 65 °C), Cr wet etching for 8 s (CEP-200 chrome etchant), and ultraviolet ozone plasma cleaning of PMMA residues on Au surface for 10 min at 150 °C.

Optical Measurements. The photoemission of STM-excited plasmon was captured by an electron-multiplying coupled-charge device (EMCCD, Princeton Instruments, ProEM$^+$, 512B Excelon 3, multiplication gain 1000×) camera at the Fourier plane (i.e., back focal plane) through an objective lens, tube lens and Bertrand lens. A 100× oil-immersion objective lens with a numerical aperture (NA) of 1.30 was used. As shown in Figure S4, the optical spectrum of the STM-excited plasmon was measured by an Andor spectrometer with a CCD camera model of "Newton DU920P−BV", which was thermo-electrically cooled down to −85 °C. The grating used in the spectrometer has 300 lines per mm. The PtIr probe is placed on the 5 μm pitch 1D cavity with a tunneling current of 50 nA, an integration time of 300 s for the spectrometer measurement, and a bias voltage of 2.5 and 2.0 V, respectively. The measured spectrum with the STM probe far away from the sample surface is denoted as "retract" to show the background level. Moreover, for the measurements of directionality factor as shown in Figure 4b,c were determined by taking the intensity ratio between the SPP propagating toward left versus right, in the zeroth-order plasmon ring of the Fourier plane. The SPP intensity data was obtained through averaging over an arc angle of 15° with 42 pixels so as to reduce the noise (as shown by the purple colored dash lines in Figure 4c). As reported in the literature,[37] the relative humidity level will affect the signal intensity from the STM-excited plasmons. In our current STM experimental setup, besides the central air condition system, we did not have an additional humidity control, and the relative humidity level was measured to be around 42%.

Numerical Simulations. Finite-difference time-domain (FDTD) simulations were performed using commercial software (Lumerical FDTD Solutions). A vertically polarized dipole source was used to model tunneling current between the STM probe and Au surface, where the dipole source emitting at the free-space wavelength of 700 nm was placed only a short distance of 1.5 nm above Au surface. To increase the computation speed and ensure the simulation accuracy, a nonuniform meshing scheme has been used, where the minimum and maximum mesh sizes are chosen at $\lambda/140$ near the gap edge region and $\lambda/20$ for the 1D cavity central region, respectively. The dielectric constants of Au, Cr, ITO, and glass are taken from Palik's handbook.[38] The thickness of ITO and Cr were 130 and 20 nm, respectively, throughout the manuscript.

■ ASSOCIATED CONTENT

Supporting Information

(S1) Fabrication process of the periodic Au 1D cavity using electron beam lithography. (S2) FDTD simulation of the SPP interference fringes when a *z*-polarized dipole source is placed at the central position of an Au stripe. (S3) Numerical analysis of the SPP "reflection" from a single edge of a semi-infinite Au film. (S4) Spectrum measurement when the PtIr probe is on the 5 μm pitch 1D-cavity. (S5) Line-scan profile of the simulated electric field intensity $|E|^2$ for Figure 3d when the dipole source is placed at $x_p = -250$ nm. (S6) Numerical simulation of the far-field emission characteristic so as to demonstrate the directionality correlation between near-field SPPs and far-field emissions through the cavity gaps. (S7) Numerical simulation of plasmons propagating on an Au 1D cavity with a pitch of 1 μm as a function of the dipole position. This material is available free of charge via the Internet at http://pubs.acs.org.

■ AUTHOR INFORMATION

Corresponding Author

*E-mail: joel_yang@sutd.edu.sg.

Present Address

[§]Department of Electrical Engineering and Computer Science, Massachusetts Institute of Technology, 77 Massachusetts Avenue, Cambridge, Massachusetts 02139, U.S.A. (D.Z.).

Notes

The authors declare no competing financial interest.

■ ACKNOWLEDGMENTS

We would like to acknowledge the funding support from Agency for Science, Technology and Research (A*STAR) Young Investigatorship (Grant No. 0926030138), SERC (Grant No. 092154099), and National Research Foundation Grant Award No. NRF-CRP 8-2011-07. H.-S. Chu would like to acknowledge the support of the A*STAR Computational Resource Centre through the use of its high performance computing facilities.

■ REFERENCES

(1) Maier, S. A. *Plasmonics: Fundamentals and Applications*; Springer: New York, 2007.

(2) Oulton, R. F.; Sorger, V. J.; Genov, D. A.; Pile, D. F. P.; Zhang, X. A hybrid plasmonic waveguide for subwavelength confinement and long-range propagation. *Nat. Photonics* **2008**, *2*, 496−500.

(3) Gramotnev, D. K.; Bozhevolnyi, S. I. Plasmonics beyond the diffraction limit. *Nat. Photonics* **2010**, *4*, 83−91.

(4) Huang, K. C. Y.; Seo, M.-K.; Sarmiento, T.; Huo, Y.; Harris, J. S.; Brongersma, M. L. Electrically driven subwavelength optical nanocircuits. *Nat. Photonics* **2014**, *8*, 244−249.

(5) Volkov, V. S.; Bozhevolnyi, S. I.; Rodrigo, S. G.; Martín-Moreno, L.; García-Vidal, F. J.; Devaux, E. s.; Ebbesen, T. W. Nanofocusing with channel plasmon polaritons. *Nano Lett.* **2009**, *9*, 1278−1282.

(6) Ropers, C.; Neacsu, C. C.; Elsaesser, T.; Albrecht, M.; Raschke, M. B.; Lienau, C. Grating-coupling of surface plasmons onto metallic tips: A nanoconfined light source. *Nano Lett.* **2007**, *7*, 2784−2788.

(7) Ozbay, E. Plasmonics: Merging photonics and electronics at nanoscale dimensions. *Science* **2006**, *311*, 189−193.

(8) Liu, Y.; Palomba, S.; Park, Y.; Zentgraf, T.; Yin, X.; Zhang, X. Compact magnetic antennas for directional excitation of surface plasmons. *Nano Lett.* **2012**, *12*, 4853−4858.

(9) Huang, X.; Brongersma, M. L. Compact aperiodic metallic groove arrays for unidirectional launching of surface plasmons. *Nano Lett.* **2013**, *13*, 5420−5424.

DOI: 10.1021/ph5004303
ACS Photonics 2015, 2, 385−391

(10) Baron, A.; Devaux, E.; Rodier, J.-C.; Hugonin, J.-P.; Rousseau, E.; Genet, C.; Ebbesen, T. W.; Lalanne, P. Compact antenna for efficient and unidirectional launching and decoupling of surface plasmons. *Nano Lett.* **2011**, *11*, 4207−4212.
(11) Lopez-Tejeira, F.; Rodrigo, S. G.; Martin-Moreno, L.; Garcia-Vidal, F. J.; Devaux, E.; Ebbesen, T. W.; Krenn, J. R.; Radko, I. P.; Bozhevolnyi, S. I.; Gonzalez, M. U.; Weeber, J. C.; Dereux, A. Efficient unidirectional nanoslit couplers for surface plasmons. *Nat. Phys.* **2007**, *3*, 324−328.
(12) Rodríguez-Fortuño, F. J.; Marino, G.; Ginzburg, P.; O'Connor, D.; Martínez, A.; Wurtz, G. A.; Zayats, A. V. Near-field interference for the unidirectional excitation of electromagnetic guided modes. *Science* **2013**, *340*, 328−330.
(13) Vercruysse, D.; Sonnefraud, Y.; Verellen, N.; Fuchs, F. B.; Di Martino, G.; Lagae, L.; Moshchalkov, V. V.; Maier, S. A.; Van Dorpe, P. Unidirectional side scattering of light by a single-element nanoantenna. *Nano Lett.* **2013**, *13*, 3843−3849.
(14) Lin, J.; Mueller, J. P. B.; Wang, Q.; Yuan, G.; Antoniou, N.; Yuan, X.-C.; Capasso, F. Polarization-controlled tunable directional coupling of surface plasmon polaritons. *Science* **2013**, *340*, 331−334.
(15) Berndt, R.; Gimzewski, J. K.; Johansson, P. Inelastic tunneling excitation of tip-induced plasmon modes on noble-metal surfaces. *Phys. Rev. Lett.* **1991**, *67*, 3796−3799.
(16) Berndt, R.; Gaisch, R.; Schneider, W. D.; Gimzewski, J. K.; Reihl, B.; Schlittler, R. R.; Tschudy, M. Atomic resolution in photon emission induced by a scanning tunneling microscope. *Phys. Rev. Lett.* **1995**, *74*, 102−105.
(17) Lutz, T.; Große, C.; Dette, C.; Kabakchiev, A.; Schramm, F.; Ruben, M.; Gutzler, R.; Kuhnke, K.; Schlickum, U.; Kern, K. Molecular orbital gates for plasmon excitation. *Nano Lett.* **2013**, *13*, 2846−2850.
(18) Walters, R. J.; van Loon, R. V. A.; Brunets, I.; Schmitz, J.; Polman, A. A silicon-based electrical source of surface plasmon polaritons. *Nat. Mater.* **2010**, *9*, 21−25.
(19) Fan, P.; Colombo, C.; Huang, K. C. Y.; Krogstrup, P.; Nygård, J.; Fontcuberta i Morral, A.; Brongersma, M. L. An electrically-driven GaAs nanowire surface plasmon source. *Nano Lett.* **2012**, *12*, 4943−4947.
(20) Li, J.; Wei, H.; Shen, H.; Wang, Z.; Zhao, Z.; Duan, X.; Xu, H. Electrical source of surface plasmon polaritons based on hybrid Au-GaAs QW structures. *Nanoscale* **2013**, *5*, 8494−8499.
(21) Neutens, P.; Lagae, L.; Borghs, G.; Van Dorpe, P. Electrical excitation of confined surface plasmon polaritons in metallic slot waveguides. *Nano Lett.* **2010**, *10*, 1429−1432.
(22) Koller, D. M.; Hohenau, A.; Ditlbacher, H.; Galler, N.; Reil, F.; Aussenegg, F. R.; Leitner, A.; List, E. J. W.; Krenn, J. R. Organic plasmon-emitting diode. *Nat. Photonics* **2008**, *2*, 684−687.
(23) Rai, P.; Hartmann, N.; Berthelot, J.; Arocas, J.; Colas des Francs, G.; Hartschuh, A.; Bouhelier, A. Electrical excitation of surface plasmons by an individual carbon nanotube transistor. *Phys. Rev. Lett.* **2013**, *111*, 026804.
(24) Marty, R.; Girard, C.; Arbouet, A.; Francs, G. C. d. Near-field coupling of a point-like dipolar source with a thin metallic film: Implication for STM plasmon excitations. *Chem. Phys. Lett.* **2012**, *532*, 100−105.
(25) Bharadwaj, P.; Bouhelier, A.; Novotny, L. Electrical excitation of surface plasmons. *Phys. Rev. Lett.* **2011**, *106*, 226802.
(26) Zhu, D.; Dong, Z.; Chu, H.-S.; Akimov, Y. A.; Yang, J. K. W. Image dipole method for the beaming of plasmons from point sources. *ACS Photonics* **2014**, *1*, 1307−1312.
(27) Wang, T.; Boer-Duchemin, E.; Comtet, G.; Moal, E. L.; Dujardin, G.; Drezet, A.; Huant, S. Plasmon scattering from holes: From single hole scattering to Young's experiment. *Nanotechnology* **2014**, *25*, 125202.
(28) Le Moal, E.; Marguet, S.; Rogez, B.; Mukherjee, S.; Dos Santos, P.; Boer-Duchemin, E.; Comtet, G.; Dujardin, G. An electrically excited nanoscale light source with active angular control of the emitted light. *Nano Lett.* **2013**, *13*, 4198−4205.
(29) Wang, T.; Boer-Duchemin, E.; Zhang, Y.; Comtet, G.; Dujardin, G. Excitation of propagating surface plasmons with a scanning tunnelling microscope. *Nanotechnology* **2011**, *22*, 175201.
(30) Zhang, Y.; Boer-Duchemin, E.; Wang, T.; Rogez, B.; Comtet, G.; Le Moal, E.; Dujardin, G.; Hohenau, A.; Gruber, C.; Krenn, J. R. Edge scattering of surface plasmons excited by scanning tunneling microscopy. *Opt. Express* **2013**, *21*, 13938−13948.
(31) Umeno, T.; Nishitani, R.; Kasuya, A.; Nishina, Y. Isochromat photon map induced by scanning tunneling microscopy from gold particles. *Phys. Rev. B* **1996**, *54*, 13499−13501.
(32) Wang, T.; Comtet, G.; Le Moal, E.; Dujardin, G.; Drezet, A.; Huant, S.; Boer-Duchemin, E. Temporal coherence of propagating surface plasmons. *Opt. Lett.* **2014**, *39*, 6679−6682.
(33) Wang, T. *Excitation électrique de plasmons de surface avec un microscope à effet tunnel*; Université Paris XI: Paris, France, 2012.
(34) Sorger, V. J.; Oulton, R. F.; Ma, R.-M.; Zhang, X. Toward integrated plasmonic circuits. *MRS Bull.* **2012**, *37*, 728−738.
(35) Kumar, K.; Duan, H. G.; Hegde, R. S.; Koh, S. C. W.; Wei, J. N.; Yang, J. K. W. Printing colour at the optical diffraction limit. *Nat. Nanotechnol.* **2012**, *7*, 557−561.
(36) Duan, H. G.; Hu, H. L.; Hui, H. K.; Shen, Z. X.; Yang, J. K. W. Free-standing sub-10 nm nanostencils for the definition of gaps in plasmonic antennas. *Nanotechnology* **2013**, *24*, 185301.
(37) Boyle, M. G.; Mitra, J.; Dawson, P. The tip−sample water bridge and light emission from scanning tunnelling microscopy. *Nanotechnology* **2009**, *20*, 335202.
(38) Palik, E. D. *Handbook of Optical Constants*. Academic Press: New York, 1984.

DOI: 10.1021/ph5004303
ACS Photonics 2015, 2, 385−391